



Published in final edited form as:

*Nat Genet.* ; 44(2): 165–169. doi:10.1038/ng.1041.

## Frequent somatic *MAP3K5* and *MAP3K9* mutations in metastatic melanoma identified by exome sequencing

Mitchell S Stark<sup>1,\*</sup>, Susan L Woods<sup>1,\*</sup>, Michael G Gartside<sup>1,\*</sup>, Vanessa F Bonazzi<sup>1,\*</sup>, Ken Dutton-Regester<sup>1,2,\*</sup>, Lauren G Aoude<sup>1,3</sup>, Donald Chow<sup>5</sup>, Chris Sereduk<sup>5</sup>, Natalie M Niemi<sup>8</sup>, Nanyun Tang<sup>5</sup>, Jonathan J Ellis<sup>6</sup>, Jeffrey Reid<sup>4</sup>, Victoria Zismann<sup>5</sup>, Sonika Tyagi<sup>1</sup>, Donna Muzny<sup>4</sup>, Irene Newsham<sup>4</sup>, YuanQing Wu<sup>4</sup>, Jane M Palmer<sup>1</sup>, Thomas Pollak<sup>1</sup>, David Youngkin<sup>5</sup>, Bradford R Brooks<sup>8</sup>, Catherine Lanagan<sup>1</sup>, Christopher W Schmidt<sup>1</sup>, Bostjan Kobe<sup>6</sup>, Jeffrey P MacKeigan<sup>8</sup>, Hongwei Yin<sup>5</sup>, Kevin M Brown<sup>5,7</sup>, Richard Gibbs<sup>4</sup>, Jeffrey Trent<sup>5,8</sup>, and Nicholas K Hayward<sup>1,†</sup>

<sup>1</sup>Queensland Institute of Medical Research, Brisbane, QLD 4006, Australia

<sup>2</sup>Queensland University of Technology, Brisbane QLD 4000, Australia

<sup>3</sup>School of Medicine, University of Queensland, Brisbane, QLD 4072, Australia

<sup>4</sup>Baylor College of Medicine, Houston, TX 77030, USA

<sup>5</sup>Translational Genomics Research Institute, Phoenix, AZ 85004, USA

<sup>6</sup>School of Chemistry and Molecular Biosciences, Institute for Molecular Biosciences and Centre for Infectious Diseases Research, University of Queensland, Brisbane, QLD 4072, Australia

<sup>7</sup>National Cancer Institute, MD 20892, USA

<sup>8</sup>Van Andel Research Institute, Grand Rapids, MI 49503, USA

### Abstract

We sequenced 8 melanoma exomes to identify novel somatic mutations in metastatic melanoma. Focusing on the MAP3K family, we found that 24% of melanoma cell lines have mutations in the protein-coding regions of either *MAP3K5* or *MAP3K9*. Structural modelling predicts that mutations in the kinase domain may affect the activity and regulation of MAP3K5/9 protein

Users may view, print, copy, download and text and data- mine the content in such documents, for the purposes of academic research, subject always to the full Conditions of use: [http://www.nature.com/authors/editorial\\_policies/license.html#terms](http://www.nature.com/authors/editorial_policies/license.html#terms)

<sup>†</sup>To whom correspondence should be addressed. [nick.hayward@qimr.edu.au](mailto:nick.hayward@qimr.edu.au).

\*These authors contributed equally

**URLs** Catalogue of Somatic Mutations in Cancer COSMIC, <http://www.sanger.ac.uk/genetics/CGP/cosmic/>;

**Accession codes** *MAP3K5*, NM\_005923; *MAP3K8*, NM\_005204; *MAP3K9*, NM\_033141; MAP3K5 kinase domain, PDB ID 2CLQ; MAP3K9 kinase domain PDB ID 3DTC; kinase domain with ATP and a substrate bound, PDB ID 2PHK

### Author Contributions

N.K.H., K.M.B., R.G. and J.T. devised the study. M.S.S., M.G.G., K.D-R., S.T., J.R., D.M., I.N. and Y.W. performed the exome sequencing and analysed the sequencing data. S.L.W., M.G.G., V.F.B., B.R.B., D.C., N.M.N., J.P.M., T.P. and H.Y. produced and analysed the functional data. M.G.G., L.A.G., K.D-R., V.Z. and D.Y. carried out confirmatory sequencing. C.W.S. and C.L. established the melanoma cell line panel and provided the fresh melanoma tumors. J.M.P. extracted and collated clinical records of the melanoma patients. M.S.S., S.L.W., M.G.G., V.F.B., J.P.M., H.Y. and N.K.H. wrote the manuscript. J.J.E. and B.K. performed protein modelling. D.C., C.S., N.T. and H.Y. performed the TMZ/siRNA sensitization studies and RT-PCR. All authors read and approved the final manuscript.

kinases. The position of the mutations and loss of heterozygosity of *MAP3K5* and *MAP3K9* in 85% and 67% of melanoma samples, respectively, together suggest that the mutations are likely inactivating. *In vitro* kinase assay shows reduction in kinase activity in MAP3K5 I780F and MAP3K9 W333X mutants. Overexpression of *MAP3K5* or *MAP3K9* mutant in HEK293T cells reduces phosphorylation of downstream MAP kinases. Attenuation of MAP3K9 function in melanoma cells using siRNA leads to increased cell viability after temozolomide treatment, suggesting that decreased MAP3K pathway activity can lead to chemoresistance in melanoma.

---

There are no long-lasting effective treatments for disseminated melanoma; however, recent developments in molecularly-targeted therapies have shown success in short term progression-free survival and the reduction of tumour burden<sup>1</sup>. The recent advent of next-generation sequencing (NGS) has enabled the identification of cancer associated mutations in an unbiased manner. These mutation catalogs have enormous potential for understanding the molecular basis of disease and identifying novel therapeutic targets. Further characterizing the pathways involved in the etiology of melanoma will help guide development of new treatments for this disease.

Utilising whole-exome capture, we sequenced 8 melanoma cell lines (Supplementary Table 1) and their matched normal lymphoblastoid cell lines (LCLs) using two NGS platforms (Illumina GAI or Life Technologies SOLiD) and mapped reads with platform appropriate alignment programs<sup>2</sup>. Our analysis schema is shown in Supplementary Fig.1. To maximise finding *bone fide* mutations we applied strict filtering criteria (described in Supplementary Fig.1 and 2) to minimize the false positive rate without overly inflating the false negative rate. Comparing Illumina SNP array data<sup>3</sup> with variant calls from the exome data yielded >99.5% concordance for each sample, thus achieving a mean false negative rate of ~0.45%. Overall, 3,215 somatic alterations were identified; range 243-523 per sample (Supplementary Table 2). Of these, 1,076 were synonymous (silent) mutations and 2,139 were predicted to alter protein structure (range 175-326 per sample), comprising: 1,925 missense, 122 nonsense, 32 splice-site and 64 small insertion/deletion mutations (Supplementary Table 2). The ratio of non-synonymous to synonymous changes (N:S ratio) was 1.9:1, which is not higher than the N:S ratio of 2.5:1 predicted for non-selected passenger mutations,<sup>3</sup> indicating that most of the mutations are likely to be passengers rather than drivers. Recent exome analysis of 14 metastatic melanomas found a similarly low (2.0:1) N:S ratio.<sup>4</sup> Analysis of the mutation spectrum showed the proportion of C>T/G>A transitions was greater than the numbers of other nucleotide substitutions (4.1:1) (Supplementary Fig. 2). We observed 17 tandem mutations, including 10 CC>TT/GG>AA alterations, which taken together, is consistent with the mutation signature associated with ultraviolet light exposure<sup>5</sup>.

Of the 1740 genes found to have protein-altering changes (Supplementary Table 3), 446 were reported to be mutated in a recent exome analysis of melanoma<sup>4</sup> and 166 have mutations documented in the COSMIC database<sup>6</sup>. The overlap between our dataset and these two other sources revealed 58 genes commonly mutated in melanoma, suggesting many are potentially 'drivers' of melanoma pathogenesis (Supplementary Table 3). We verified mutations in key melanoma-associated genes, including: *GRIN2A*<sup>4</sup> (2/8 samples),

*TRRAP*<sup>4</sup> (2/8 samples), *ADAM29*<sup>7</sup> (2/8 samples), *ADAMTS18*<sup>8</sup> (2/8 samples) and *ERBB4*<sup>9</sup> (2/8 samples) (Supplementary Tables 3 and 4). We also confirmed prevalent mutations of many G protein-coupled receptor family members<sup>10</sup> (Supplementary Table 3). Novel genes included *SLC2A12* (3/8 samples) and *RGSL1* (3/8 samples), both with a high frequency (38%) of mutations in the discovery screen. Mutations were found in 22 genes lying in previously described regions of homozygous deletion (Supplementary Table 5), including *PTPRD*<sup>11</sup> (5 mutations in 4 samples), a putative tumor suppressor gene for melanoma and glioblastoma<sup>12</sup>.

The mitogen-activated protein kinase (MAPK) pathway plays an important role in melanoma genesis,<sup>13,14</sup> where *BRAF*, encoding a MAP3K, is the most commonly mutated gene<sup>15</sup>. Considering the importance of *BRAF* in melanoma, along with the impact that mutation of this kinase has on the efficacy of some new molecularly-targeted therapies for melanoma, we focused our attention on other mutated MAP3K family members.

*MAP3K5*, *MAP3K8* and *MAP3K9* each showed somatic mutations in 1/8 samples. We validated those in *MAP3K5* and *MAP3K9* but the *MAP3K8* mutation was found to be a false positive. A prevalence screen revealed 8/85 melanoma cell lines with somatic non-synonymous mutations in *MAP3K5* (8 mutations) and 13/85 cell lines with mutations in *MAP3K9* (total of 18 mutations) (Fig. 1). Overall, *MAP3K5* and *MAP3K9* were mutated in 9% and 15% of melanoma cell lines respectively and mutation of either gene occurred in 24% of samples. Matched tumor DNA was sequenced, and *MAP3K5* or *MAP3K9* mutations validated in all but one sample (Supplementary Table 6), indicating the mutations were not the result of cell culturing. For the one discordant pair it is possible the W333X mutation in *MAP3K9* arose in the cell line *in vitro*, or that the cell line was derived from a sub-population of tumor cells that carried the mutation but was too low to detect by sequencing of the tumor. With the exception of one cell line, mutations in *MAP3K5* or *MAP3K9* were mutually exclusive (Supplementary Table 6), suggesting they may target the same pathway. Four *MAP3K9* (chromosome 14) mutations and five *MAP3K5* (chromosome 6) were homozygous, suggesting loss of somatic heterozygosity (LOH) at these loci. Analysis of SNP array data for these and other melanoma cell lines<sup>12</sup> and K.D-R, N.K.H unpublished data confirmed this supposition and showed that 98/115 (85%) and 77/115 (67%) samples had LOH for *MAP3K5* or *MAP3K9* respectively (Supplementary Fig 3). LOH included loss of chromosome 6 (15/98; 15%), and whole q-arm loss encompassing *MAP3K5* (18/98; 18%) or *MAP3K9* (chromosome 14) respectively (46/77; 60%). Areas of regional LOH that included up to 5 Mb on either side of *MAP3K5* (39/98; 40%) and *MAP3K9* (9/77; 12%) also occurred. Additionally, *MAP3K5* (26/98; 27%) and *MAP3K9* (22/77; 29%) were often found in focal areas of LOH encompassing only a small number of genes. The high rate of LOH, the distribution of mutations along the entire length of each gene and the identification of a nonsense mutation in *MAP3K9*, suggests the mutations are inactivating. Interestingly, along with homozygous mutations, a number of heterozygous mutations were identified. We propose, that in a similar fashion to genes such as *TP53* and *PTEN*<sup>16</sup> and *CDKN1B*<sup>17</sup>, these heterozygous mutations result in reduced gene function via haploinsufficiency and reduction of wild type protein. Mutations in *MAP3K5* and *MAP3K9* were not correlated with mutations/deletions of *BRAF*, *NRAS*, *CDKN2A*, *PTEN*, or *TP53* (Supplementary Table 6).

Levels of *MAP3K5* and *MAP3K9* transcripts did not correlate with mutation status (Supplementary Fig. 5 and Supplementary Table 7), suggesting the mutations do not grossly affect mRNA expression and stability.

We analysed the available three-dimensional protein structures to provide insight to whether the *MAP3K5* or *MAP3K9* mutations may have an effect on structure or kinase activity (Fig. 2). This modelling suggested that the *MAP3K5* I780F mutation is likely to affect the packing of helices in the kinase domain (Fig. 2a). The *MAP3K9* W333X mutation results in the production of a truncated non-functional kinase domain that is unlikely to be functional. The R160 residue in *MAP3K9* forms hydrogen bonds with E167 that would be disrupted by the mutation to cysteine (R160C), while the *MAP3K9* P263L mutation is predicted to increase conformational flexibility in the corresponding loop (Fig. 2b). The *MAP3K9* E319 residue forms hydrogen bonds with R393 and the mutation to lysine will disrupt this interaction, potentially altering the kinase domain surface and affecting interactions with other molecules.

To confirm these predicted changes, we performed *in vitro* kinase assays using cDNA constructs containing mutations suggestive of decreased kinase activity in both *MAP3K5* (E663K and I780F) and *MAP3K9* (W333X and the previously described<sup>18</sup> kinase dead mutation, K171A). We over-expressed these mutants in mammalian cells and, upon immunoprecipitation, assayed kinase activity. Figures 3a and b show wild type *MAP3K9* and *MAP3K5* have robust kinase activity against myelin basic protein (MBP), as well as substantial autophosphorylation. *MAP3K9* K171A and W333X mutants showed a 92% and 95% reduction in kinase activity against MBP relative to the wild type enzyme ( $p < 0.001$ ). Additionally, *MAP3K5* I780F almost completely abolishes kinase activity (93% reduction relative to wild type,  $p < 0.01$ ), while the mutant E663K had lesser yet statistically significant effects on MBP phosphorylation (30% reduction relative to wild type,  $p < 0.05$ ).

Cellular stresses including UV radiation and oxidative stress activate *MAP3K5* leading to downstream activation of the JNK and p38 MAPK effector pathways and context-dependent induction of apoptosis, differentiation, survival or senescence<sup>19,20</sup> (Supplementary Fig. 4). While less intensively studied, the *MAP3K9* transcript is widely expressed<sup>21</sup> and activation results in downstream signaling through MAP2K4 and JNK, with the effect on other MAPK effector modules currently unknown<sup>18</sup>. To further investigate the functional consequences of *MAP3K5*/*MAP3K9* mutations we assessed key components of the downstream signaling pathways after introduction of either the wild-type or mutant kinases into cells. Given the well established difficulty in transfecting melanoma cell lines, in addition to their often perturbed MAPK signaling, we chose HEK293T cells as a model system due to their high inherent transfection efficiency and low constitutive MAPK signaling levels. Exogenous expression of *MAP3K5* led to activation of this protein by phosphorylation, with downstream activation of the MAP2K4/7-JNK and p38 pathways when compared to control EGFP expression (Fig. 4a). Similar levels of *MAP3K9* and *MAP3K5* expression were obtained as observed using the Myc-epitope antibody on both proteins in a Western blot (data not shown). However we observed differential activation of downstream MAPKs as expression of *MAP3K9* led to activation of MAP2K4/7-JNK and not the p38 module (Fig. 4b). Expression of *MAP3K9*, and to a lesser degree *MAP3K5*, also activated MEK1/2 and

ERK (Fig. 4a and b). We engineered the two mutations into MAP3K5 most likely to affect protein function, one in the kinase domain (I780F, Fig. 2a) and one adjacent to the kinase domain that introduces a charge change (E663K, Fig. 1). Their expression resulted in reduced phosphorylation of MAP3K5 in the I780F mutant when normalised for the amount of total MAP3K5 expressed, and in JNK signaling, with decreased phospho-MEK1/2 (P-MEK1/2) downstream of both mutants (Fig. 4a). Expression of either mutant MAP3K9 protein (W333X and control K171A<sup>18</sup>) resulted in decreased signaling through MAP2K4/7-JNK and MEK1/2-ERK (Fig. 4b) consistent with the reduction in kinase activity of these mutants shown *in vitro* (Fig. 3).

Until recently, melanoma was notoriously refractory to chemotherapeutic intervention and understanding the mechanisms of this chemoresistance is vital to improving the outlook for patients with metastatic disease. Temozolomide (TMZ) is an alkylating agent that has been reported to modestly increase progression-free survival as a single-agent in randomised Phase III trials<sup>22</sup>. In a high throughput siRNA screen for sensitizers to TMZ treatment (unpublished data), we noted that knockdown of MAP3K9 resulted in increased resistance, rather than sensitivity, to TMZ treatment. As the mutations that we have examined appear to decrease MAP3K5/9 activity and downstream signaling, we examined the effect of attenuating wild-type MAP3K5/9 in melanoma cells, specifically, whether decreased expression of wild-type MAP3K5/9 can contribute to TMZ-chemoresistance. Transfection of melanoma cell lines UACC903 and UACC647 with three independent siRNAs targeting either *MAP3K5* (data not shown) or *MAP3K9* (Fig. 5a) resulted in decreased target mRNA expression to at least 60% of the level observed in scrambled-control siRNA-treated cells. Treatment of control siRNA transfected melanoma cells with TMZ resulted in much decreased viability (Fig. 5 bi,ii), consistent with apoptosis being the predominant form of cell death in melanoma cell lines after TMZ treatment<sup>23</sup>. For the two cell lines tested, siRNA knockdown of *MAP3K9* alone reduced cell viability in UACC903 which contrasts with UACC647 where siRNA treatment alone has little if any effect. However, upon combination of both siRNA knockdown and TMZ, both cell lines exhibit a resistance phenotype as evidenced by increased cell viability in the presence of both agents compared with drug alone (Fig. 5 bi,ii). Similar experiments conducted for *MAP3K5* did not show a statistically significant increase in cell viability following combined siRNA and TMZ treatment (data not shown). This suggests that attenuated MAP3K9 activity can contribute to chemotherapeutic resistance in melanoma.

In conclusion, we have shown almost mutually exclusive mutation of *MAP3K5* and *MAP3K9* in approximately 24% of melanomas, which occurs independently of activating mutations in *BRAF* or *NRAS*. Together with the high rates of LOH at these two loci, aberrations of these genes represent a very common event in melanoma. Given that homozygous deletion of *MAP3K5* results in increased tumor initiation in a carcinogen induced model of skin cancer<sup>20</sup>, that MAP3K9 regulates apoptosis via MAP2K4/7-JNK<sup>24</sup>, and that diminished activation of JNK1 can result in enhanced survival of tumor cells<sup>25</sup>, our data indicate that abrogation of this signaling axis (Supplementary Fig. 4) is important for melanoma development. Reactivation of the signaling pathways downstream of mutant MAP3K5 or MAP3K9 might thus be therapeutically advantageous in treating this disease.

## Supplementary Material

Refer to Web version on PubMed Central for supplementary material.

## Acknowledgments

This work was funded through grants from the National Health and Medical Research Council of Australia, the Australian Centre for Vaccine Development, the National Cancer Institute (5R01CA129447, PI Trent), National Cancer Institute, Division of Cancer Epidemiology and Genetics (PI Brown) and a charitable donation by Francis Najafi. The authors would like to acknowledge Mr. Meraj Aziz for data processing Michelle Kassner for technical support and Jose-Carlos Deza for graphics support.

## References

1. Flaherty KT, et al. Inhibition of mutated, activated BRAF in metastatic melanoma. *N Engl J Med*. 2010; 363:809–819. [PubMed: 20818844]
2. Materials and Methods are available as supporting material on Nature Genetics Online.
3. Sjoblom T, et al. The consensus coding sequences of human breast and colorectal cancers. *Science*. 2006; 314:268–274. [PubMed: 16959974]
4. Wei X, et al. Exome sequencing identifies GRIN2A as frequently mutated in melanoma. *Nat Genet*. 2011; 43:442–446. [PubMed: 21499247]
5. Greenman C, et al. Patterns of somatic mutation in human cancer genomes. *Nature*. 2007; 446:153–158. [PubMed: 17344846]
6. Bamford S, et al. The COSMIC (Catalogue of Somatic Mutations in Cancer) database and website. *Br J Cancer*. 2004; 91:355–358. [PubMed: 15188009]
7. Wei X, et al. Analysis of the disintegrin-metalloproteinases family reveals ADAM29 and ADAM7 are often mutated in melanoma. *Hum Mutat*. 2011; 32:E2148–2175. [PubMed: 21618342]
8. Wei X, et al. Mutational and functional analysis reveals ADAMTS18 metalloproteinase as a novel driver in melanoma. *Mol Cancer Res*. 2010; 8:1513–1525. [PubMed: 21047771]
9. Prickett TD, et al. Analysis of the tyrosine kinome in melanoma reveals recurrent mutations in ERBB4. *Nat Genet*. 2009; 41:1127–1132. [PubMed: 19718025]
10. Prickett TD, et al. Exon capture analysis of G protein-coupled receptors identifies activating mutations in GRM3 in melanoma. *Nat Genet*. 2011 10.1038/ng.950.
11. Stark M, Hayward N. Genome-wide loss of heterozygosity and copy number analysis in melanoma using high-density single-nucleotide polymorphism arrays. *Cancer Res*. 2007; 67:2632–2642. [PubMed: 17363583]
12. Solomon DA, et al. Mutational inactivation of PTPRD in glioblastoma multiforme and malignant melanoma. *Cancer Res*. 2008; 68:10300–10306. [PubMed: 19074898]
13. Dhillon AS, Hagan S, Rath O, Kolch W. MAP kinase signalling pathways in cancer. *Oncogene*. 2007; 26:3279–3290. [PubMed: 17496922]
14. Johannessen CM, et al. COT drives resistance to RAF inhibition through MAP kinase pathway reactivation. *Nature*. 2010; 468:968–972. [PubMed: 21107320]
15. Davies H, et al. Mutations of the BRAF gene in human cancer. *Nature*. 2002; 417:949–954. [PubMed: 12068308]
16. Berger AH, Pandolfi PP. Haplo-insufficiency: a driving force in cancer. *J Pathol*. 2011; 223:137–146. [PubMed: 21125671]
17. Paige AJ. Redefining tumour suppressor genes: exceptions to the two-hit hypothesis. *Cell Mol Life Sci*. 2003; 60:2147–2163. [PubMed: 14618262]
18. Durkin JT, et al. Phosphoregulation of mixed-lineage kinase 1 activity by multiple phosphorylation in the activation loop. *Biochemistry*. 2004; 43:16348–16355. [PubMed: 15610029]
19. Takeda K, Noguchi T, Naguro I, Ichijo H. Apoptosis signal-regulating kinase 1 in stress and immune response. *Annu Rev Pharmacol Toxicol*. 2008; 48:199–225. [PubMed: 17883330]

20. Iriyama T, et al. ASK1 and ASK2 differentially regulate the counteracting roles of apoptosis and inflammation in tumorigenesis. *EMBO J.* 2009; 28:843–853. [PubMed: 19214184]
21. Bisson N, et al. Mice lacking both mixed-lineage kinase genes *Mlk1* and *Mlk2* retain a wild type phenotype. *Cell Cycle.* 2008; 7:909–916. [PubMed: 18414056]
22. Middleton MR, et al. Randomized phase III study of temozolomide versus dacarbazine in the treatment of patients with advanced metastatic malignant melanoma. *J Clin Oncol.* 2000; 18:158–166. [PubMed: 10623706]
23. Naumann SC, et al. Temozolomide- and fotemustine-induced apoptosis in human malignant melanoma cells: response related to MGMT, MMR, DSBs, and p53. *Br J Cancer.* 2009; 100:322–333. [PubMed: 19127257]
24. Xu Z, Maroney AC, Dobrzanski P, Kukekov NV, Greene LA. The MLK family mediates c-Jun N-terminal kinase activation in neuronal apoptosis. *Mol Cell Biol.* 2001; 21:4713–4724. [PubMed: 11416147]
25. She QB, Chen N, Bode AM, Flavell RA, Dong Z. Deficiency of c-Jun-NH(2)-terminal kinase-1 in mice enhances skin tumor development by 12-O-tetradecanoylphorbol-13-acetate. *Cancer Res.* 2002; 62:1343–1348. [PubMed: 11888903]

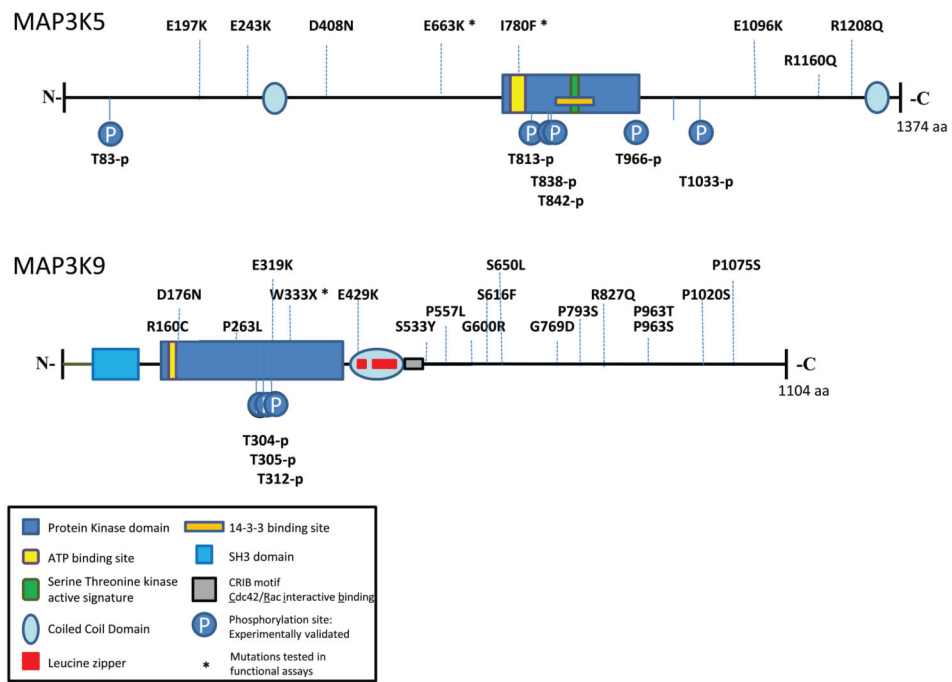


**Figure 1.** Schema depicting MAP3K5 and MAP3K9 domain structure, phosphorylation sites (below each gene) and the position of validated somatic non-synonymous mutations identified by whole-exome sequencing (above each gene).



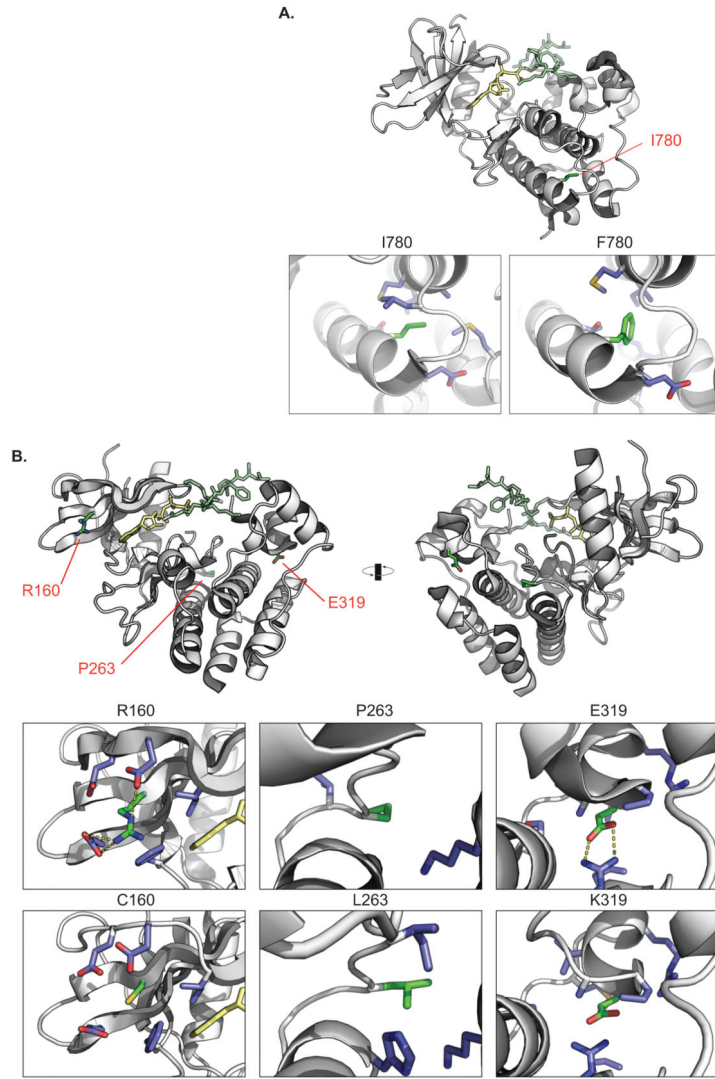


**Figure 2.** Mutations found in melanoma are predicted to affect the function or regulation of MAP3K5 and MAP3K9 kinase domains. **(a)** The top panel shows MAP3K5 kinase domain (PDB ID 2CLQ). The kinase domain was aligned with PDB ID 2PHK (not shown) to show approximate binding positions of ATP (yellow) and a substrate (light green). Bottom left panel shows wild-type I780 (green) and its surroundings; bottom right panel shows mutant F780 and its surroundings (green). **(b)** The top left panel shows MAP3K9 (PDB ID 3DTC) kinase domain. The top right panel is the same domain rotated by 180 degrees to show the location of all residues of interest. The kinase domain has been aligned with PDB ID 2PHK (not shown) to show approximate binding positions of ATP (yellow) and a substrate (green). The middle panels show the wild-type residues in green (R160, P263 and E319) and their surroundings; the bottom panels show the mutant residues in green (C160, L263 and K319). The disruption of hydrogen bonds can be seen for R160C and E319K. MAP3K9 D176N is in a disordered loop and the MAP3K5 E663 residue is not resolved in the crystal structure;

therefore, they do not appear in the diagrams. Only side chains within 5Å of the residue of interest are depicted.

Author Manuscript

Author Manuscript

Author Manuscript

Author Manuscript

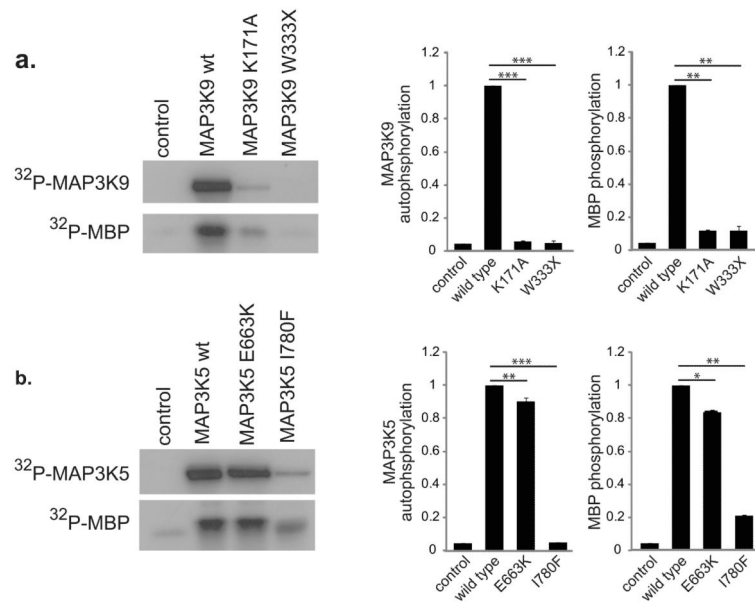


**Figure 3.**

Melanoma-associated mutations decrease the kinase activity of MAP3K9 and MAP3K5. HEK293T cells were transfected with wild type and mutant MAP3K9 (K171A and W333X) or MAP3K5 (E663K and I780F) to assess the effect of mutation on kinase activity *in-vitro*. Autophosphorylation of MAP3K9 (**a**) or MAP3K5 (**b**), and phosphorylation of the kinase substrate myelin basic protein (MBP), were measured by  $^{32}\text{P}$ - $\gamma$ ATP incorporation and quantitated using PhosphorImager. Error bars represent standard deviations; \* $p < 0.05$ , \*\* $p < 0.01$ , \*\*\* $p < 0.001$  by two-tailed Student's t-test.

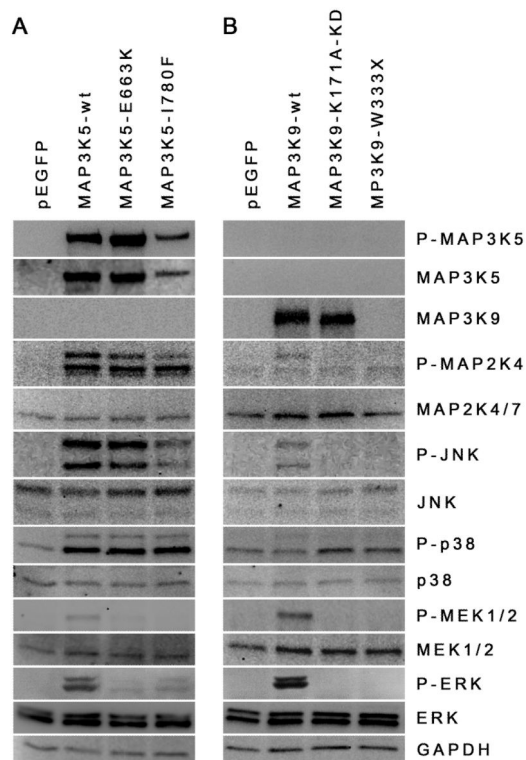


**Figure 4.** Mutation of MAP3K5 or MAP3K9 results in decreased phospho-MEK/ERK and phospho-JNK compared to wild type proteins, indicating altered downstream signaling through multiple pathways. HEK293T cell lines were transfected with expression plasmids for EGFP, wild-type or mutant MAP3K5 (**a**) or EGFP, wild-type or mutant MAP3K9 (**b**) for 48 h before analysis of protein expression and MAPK signaling by Western blot using the indicated antibodies. P-indicates the phosphorylated protein is being detected. Results are representative of three independent repeats of this experiment.

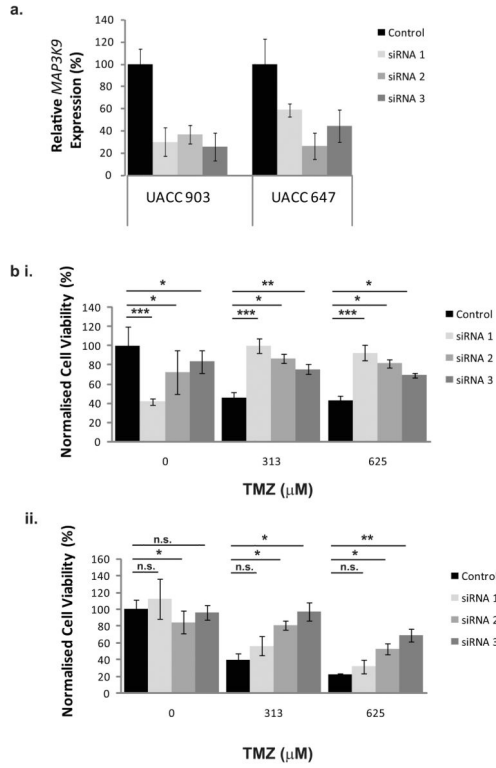


**Figure 5.** Reduced *MAP3K9* level protects melanoma cells from chemotherapeutic treatment. **(a)** Melanoma cell lines (UACC903 and UACC647) were transfected with siRNA targeting GFP (Control) or three independent siRNAs targeting *MAP3K9* (siRNA 1-3) for 120 h. Expression of *MAP3K9* determined by qRT-PCR normalized to *GAPDH* and relative to control siRNA is shown. Experiment performed in triplicate; error bars denote standard deviation. All three independent siRNAs resulted in decreased expression of *MAP3K9*. **(b)** UACC903 **(i)** and UACC647 **(ii)** cells were transfected as in a. for 24 h before treatment with the indicated dose of temozolomide (TMZ). Cell viability determined after 5 days indicated that reduced *MAP3K9* expression in the presence of TMZ resulted in a resistant phenotype.